Science of the Total Environment 888 (2023) 164250

Contents lists available at ScienceDirect

Science of the Total Environment

journal homepage: www.elsevier.com/locate/scitotenv

Effects of climate change on aquaculture site selection at a temperate estuarine system

Humberto Pereira [a,*], Ana Picado [a], Magda C. Sousa [a], Ana C. Brito [b,c], Beatriz Biguino [b], David Carvalho [a], João Miguel Dias [a]

[a] CESAM – Centre for Environmental and Marine Studies, Departamento de Física, Universidade de Aveiro, 3810–193 Aveiro, Portugal
[b] MARE – Marine and Environmental Sciences Centre/ARNET – Aquatic Research Network, Faculdade de Ciências, Universidade de Lisboa, 1749–016 Lisboa, Portugal
[c] Departamento de Biologia Vegetal, Faculdade de Ciências, Universidade de Lisboa, 1749–016 Lisboa, Portugal

HIGHLIGHTS

- Definition of five suitability classes for aquaculture exploitation.
- Best locations for aquaculture infrastructures located in the northern region of the estuary.
- Improvement in the suitability of both species production is predicted for the future.
- This work can be replicated in other estuarine systems supporting the implementation of new facilities in suitable locations.

GRAPHICAL ABSTRACT

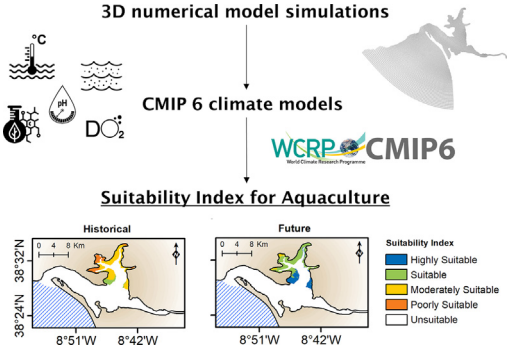

ARTICLE INFO

Editor: José Virgílio Cruz

Keywords:
Numerical modeling
Delft3D
Water quality
Sado estuary

ABSTRACT

Aquaculture is one of the food industries that most evolved in recent years in response to increased human demand for seafood products, which has led to a progressive stock threat in nature. With a high seafood consumption per capita, Portugal has been exploring its coastal systems to improve the cultivation of fish and bivalve species with high commercial value. In this context, this study aims to propose the use of a numerical model as a tool to assess the impact of climate change on aquaculture site selection in a temperate estuarine system (Sado estuary). Therefore, the Delft3D model was calibrated and validated, showing good accuracy in predicting the local hydrodynamics, transport, and water quality. Furthermore, two simulations for the historical and future conditions were performed to establish a Suitability Index capable of identifying the most appropriate sites to exploit two bivalve species (one clam and one oyster), considering both winter and summer seasons. Results suggest that the estuary's northernmost region presents the best conditions for bivalves' exploitation, with more suitable conditions during summer than winter due to the higher water temperature and chlorophyll-*a* concentrations. Regarding future projections, the model results suggest that environmental conditions will likely benefit the production of both species due to the increase in chlorophyll-*a* concentration along the estuary.

1. Introduction

Coastal transition zones, such as lagoons and estuaries, are among the most threatened areas by anthropogenic pressures, which experience frequent disturbances in tidal levels, salinity/water temperature, extreme

* Corresponding author.
E-mail address: humberto.pereira@ua.pt (H. Pereira).

http://dx.doi.org/10.1016/j.scitotenv.2023.164250
Received 20 January 2023; Received in revised form 13 May 2023; Accepted 14 May 2023
Available online 16 May 2023

events frequency and amplitude (floods, droughts, and storm surges) (Leal Filho et al., 2022), and in water quality (eutrophication, harmful algal blooms, and hypoxia) (Robins et al., 2016). These vulnerable regions are highly productive and nutrient-rich, hosting a large diversity of habitats and aquaculture units, and therefore the study of climate change impacts in these regions becomes significant to ensure the sustainable use of marine resources.

Aquaculture is an economic activity that has proliferated in recent years. The effort to stop the extinction of some marine species (reducing their capture in the ocean) and the need to produce seafood to supply an increasing world population through sustainable practices make this industry one of the most prosperous but also challenging for the future, considering all the environmental changes expected due the climate change impacts in physical-chemical properties of marine ecosystems (Barange et al., 2014; FAO, 2022; Subasinghe et al., 2009). In Portugal, aquaculture is mainly carried out in transitional waters (estuaries and lagoons), and therefore induced climate modifications in their water quality may lead to changes in bivalve and fish production and development. Indeed, bivalve species are susceptible to changes in the physical and chemical characteristics of the surrounding water (Carroll et al., 2009; Dekker and Beukema, 1999; Helmuth et al., 2006), which can affect their abundance and distribution (Steeves et al., 2018).

Numerical models are important tools to predict climate change's impact on coastal transition zones and infer its implications on ecosystem functioning. Indeed, the effects of climate change on coastal systems have been the topic of many modeling studies (e.g., Des et al., 2020; Filgueira et al., 2016; Iglesias et al., 2022; Lopes et al., 2022; Miranda et al., 2013; Pereira et al., 2022), but only a limited number address the complex joint simulation of hydrodynamics, salt and heat transport, and water quality (e.g., Mateus and Neves, 2008; Picado et al., 2020; Rodrigues et al., 2021; Vaz et al., 2021; Xu and Hood, 2006; Xue and Chai, 2012). These studies applied numerical models to explain the effects of climate change and anthropogenic pressures on the water quality, the seasonal and diurnal water quality and ecological dynamics in a lagoon channel, the inclusion of mathematical modeling in decision processes, and the aquaculture site selection through a habitat suitability model.

The Sado estuary has an essential role in the local and national economy and is consequently under strong anthropogenic pressures. The main urban and industrial strains are located on the northern margin of the estuary (Fig. 1). However, during the summer months, due to the presence of several tourism complexes, the southern margin also undergoes high urban pressure (Coutinho, 2003; Freitas et al., 2008; Gomes, 2019). Surrounding the estuary and the Sado river are agriculture and fish farming areas. According to the Portuguese Institute for Sea and Atmosphere (IPMA) and the Directorate-General for Natural Resources, Safety, and Maritime Services (DGRM), the leading aquaculture establishments are found in the Northern region (Fig. 1), and the main shellfish species exploited here are the European Flat Oyster (*Ostrea edulis*) and the Portuguese Oyster (*Magallana angulata*).

Currently, the available information concerning the effects of climate change on aquaculture production and development is very scarce, especially in estuarine systems. Indeed, according to Biguino et al. (2023), although the number of publications on climate change has been increasing since 2000, only 0.9 % correspond to estuarine systems. Moreover, focusing on the Sado estuary and climate change, only Brito et al. (2023) conducted a study evaluating the ecological carrying capacity for bivalve production under present and future conditions.

Therefore, this work aimed to develop a 3D application for the Sado estuary based on the numerical model Delft3D to understand the possible impacts of climate change on the existing aquaculture units in the system. This model application is the first to be published that represents the three-dimensional structure of the estuary's biogeochemical dynamics. The results from one earth system model (MPI-ESM) were used as model input to study the variation of physical and water quality variables throughout the system, comparing historical (1995–2014) and future (2081–2100) periods. Subsequently, a Suitability Index was determined and mapped to identify the areas with the best capacity for aquaculture production.

2. Materials and methods

2.1. Sado estuary

The Sado estuary (Fig. 1) is one of the Portuguese most important transitional water systems due to its dimensions, socio-economic relevance, and geomorphological diversity (Brito, 2009). Located in the Setúbal peninsula, this estuarine system presents three sections with distinct characteristics: a lower area (the Bay of Setúbal near the estuary entrance), a vast intertidal zone, and the upper area located in the Eastern part of the estuary (Coutinho, 2003).

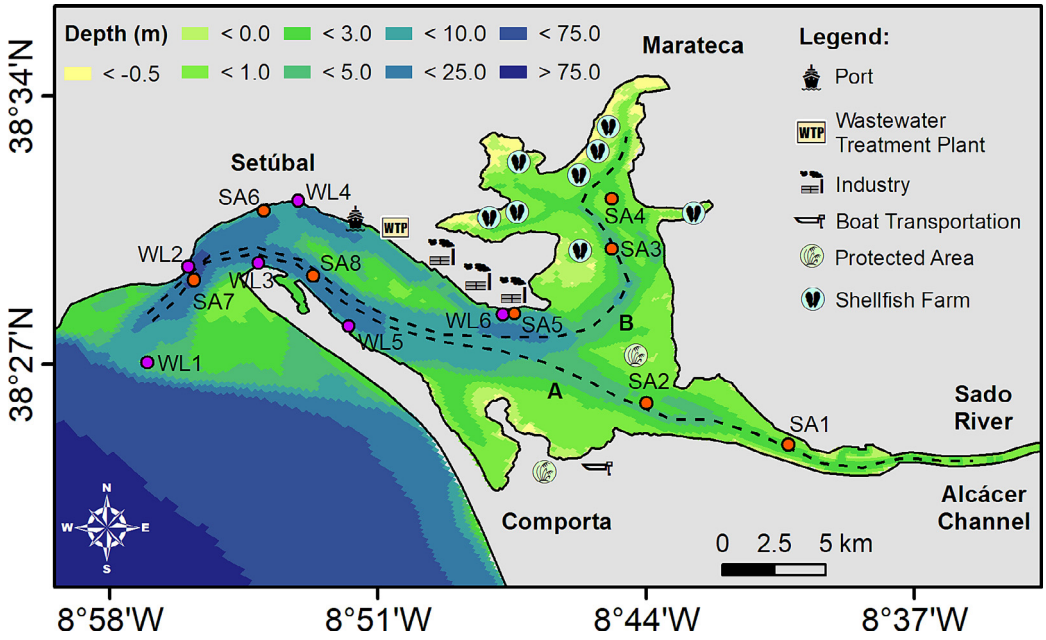

Fig. 1. Bathymetry of the Sado estuary, with the representation of sampling locations (water level (WL purple spheres) and water temperature, salinity, and water quality properties (SA orange spheres)), and two vertical transects (dashed lines A and B).

The lower estuary has a complex topography, with two large channels separated by intertidal sandbanks, and is dominated by the water coming from the ocean (Cabral, 2000; Coutinho, 2003; Ferreira et al., 2003). These two predominant flow channels have different characteristics: one northward with an average depth of 10 m and the other southward with 35 m (Coutinho, 2003; Freitas et al., 2008; Rodrigues and Quintino, 1993). The entrance of the estuary has 2 km wide.

The intertidal zone occupies 1/3 of the estuary, and the tidal effect controls the circulation here (Martins et al., 2002). The tide is semidiurnal, ranging from 0.6 m in neap tides and 1.6 m in spring tides (Martins et al., 2001). This area has a slight influence from the Marateca and Comporta creeks (Fig. 1) and is integrated into the Sado Estuary Natural Reserve, which is essentially composed of agricultural and forest areas (Freitas et al., 2007; Lillebø et al., 2011).

The upper part of the estuary, the Alcácer channel (Fig. 1), has around 30 km of extension, an average depth of 5 m, and receives the Sado river freshwater (Ferreira et al., 2003; Vale et al., 1993). The average annual flow of the river is 40 m^3s^{-1}, presenting a high seasonal variability (from 1 m^3s^{-1} in summer to 60 m^3s^{-1} in winter) (Bettencourt and Ramos, 2003; Vale et al., 1993). Under typical river flow conditions, the estuary is well mixed, although, during winter months, high discharges may cause moderate stratification in some parts of the estuary (Ferreira et al., 2003). The Marateca creek, located north of the estuary, represents 5–10 % of the total freshwater that flows to the estuary (Ferreira et al., 2003).

Physical and biochemical variables present a typical spatial gradient along the estuary. Water temperature and chlorophyll-*a* (Chl-*a*) concentration increase upstream, whereas an opposite gradient for salinity and pH is observed (Nascimento et al., 2021; Sent et al., 2021). Also, this estuarine system has a dry sub-humid Mediterranean climate, with a dry period from April to September and a humid period from October to March (Bettencourt and Ramos, 2003; Biguino et al., 2021).

2.2. Model set-up

A 3D implementation was established for the Sado estuary by applying the FLOW module and, for the first time, the WAQ module of the numerical model Delft3D (Deltares, 2021, 2014). A structured (curvilinear) spherical grid was generated based on the applications developed by Aguiar et al. (2020) and Ribeiro et al. (2016). The main differences to the previous implementations are the increase of the grid resolution (from ~1500 m to ~300 m on average in the offshore region and from ~100 m to ~80 m in the estuary body) and the inclusion of the intertidal areas in the grid. Five sigma layers were defined with a variable layer thickness.

The bathymetry of the coastal region was generated using the General Bathymetric Chart of the Oceans data (GEBCO, https://www.gebco.net/data_and_products/gridded_bathymetry_data/), and the bathymetry of the estuary was generated by compiling bathymetric data between 1964 and 2009 from the Portuguese Hydrographic Institute.

At the ocean's open boundary, it was applied 13 tidal constituents (M_2, S_2, N_2, K_2, K_1, O_1, P_1, Q_1, MF, MM, M_4, MS_4, and MN_4) retrieved from the OSU TOPEX/Poseidon 8.0 model Global Inverse Solution (https://sealevel.jpl.nasa.gov/missions/topex-poseidon/summary/) for the flow conditions. For the transport conditions, free hindcast data from the Copernicus Marine Environment Monitoring Service (CMEMS, https://marine.copernicus.eu/about/producers/ibi-mfc) on the physical and biogeochemical status, variability, and dynamics of the ocean and marine ecosystems were used. The IBI – Monitoring Forecasting Centre provides an operational marine forecasting service for the European Atlantic region, which outputs have high reliability to represent physical and biogeochemical oceanic variables and, therefore, have been used for numerical models' validation (Lorente et al., 2016; Reale et al., 2020), or for ocean boundaries in modeling studies (Declerck et al., 2019; Des et al., 2019; Sousa et al., 2018). Thus, the salinity and water temperature data were obtained from the IBI_MULTIYEAR_PHY_005_002 product, and the nutrients (ammonium (NH_4), nitrate (NO_3), and phosphate (PO_4)), pH, dissolved oxygen (DO), and Chl-*a* data from the IBI_MULTIYEAR_BGC_005_003 product. All data were obtained from the nearest points of the ocean boundary limits.

Additionally, from the European Centre for Medium-Range Weather Forecasts (ECMWF, https://www.ecmwf.int/en/forecasts/datasets/reanalysis-datasets/era5), ERA5 data was used to compute the surface air temperature, relative humidity, net radiation, wind speed, and wind direction applied in the heat flux model (absolute flux, net solar radiation) of the atmospheric interface. This heat flux model calculates evaporation internally when necessary for the heat balance (Deltares, 2021).

For the freshwater input, the two main tributaries of the estuary were considered: the Sado river and the Marateca channel. Data for fluvial discharges and water properties were retrieved from the Moinho da Gamitinha station available in the Portuguese Water Resources Information System (SNIRH, https://snirh.apambiente.pt/). Climatology for the 1990–2020 period was computed due to the data gaps in the SNIRH database. The flow's climatology was calculated with daily river flows by applying a filter that identifies and eliminates outliers (considering that an outlier is a value with a mean absolute deviation 3 scales higher than the median). Fig. SM1 shows the climatology for the flow, water temperature, and nutrients used to force the model in the fluvial boundary.

The manning values used for bottom roughness varied with bathymetry. They were derived from the values proposed by Lopes (2016) and Ribeiro et al. (2016) through a slight adjustment procedure along consecutive numerical simulations until an optimization is obtained between the model results and the observations. The background horizontal eddy viscosity and diffusivity were set to 1 and 10 m^2s^{-1}, respectively, and the background vertical eddy viscosity and diffusivity to 10^{-6} m^2s^{-1}. The k-Epsilon closure model was used for the turbulence model. A time step of 30 s was used in the flow and transport implementations.

The WAQ simulations were prepared considering variables and substances such as DO, NH_4, NO_3, PO_4, and algae (in diatom and non-diatom forms) following the implementation of Brito et al. (2023). Within these variables and substances, different processes were activated, such as the uptake of nutrients derived from algae growth, the nitrification of ammonium, the calculation of pH, and the dynamics of the DEB mussel (more detailed information regarding these processes can be found in Deltares (2018)). The activation of these variables and substances resulted in 23 physical and biological process parameters (Table SM1) adjusted along the calibration process. The WAQ simulations were performed with a time step of 30 min, five depth layers, and using the integration method 16 (Iterative solver, horizontally backward, vertically central) with the vertical Forester filter activated.

2.3. Field data

Data from monthly campaigns performed in the framework of the AQUASado project (Santos et al., 2022; Sent et al., 2021) through the years 2018 and 2019 were used to calibrate and validate the simulated water temperature, salinity, and water quality variables (DO, pH, Chl-*a*, NO_3, PO_4, and NH_4). These samplings were conducted at the surface (<1 m depth) in seven stations (SA1 to SA7) along the estuary according to its morphological characteristics and physicochemical properties (Fig. 1). Furthermore, to understand if the model can represent the vertical patterns in the Sado estuary, the water temperature and salinity data collected by Biguino et al. (2021), between September 2018 and September 2019, at stations SA6, SA7, and SA8 were also used.

2.4. Model's calibration and validation

The hydrodynamic module was calibrated with two-month numerical simulation results for 2010 (with a spin-up of 15 days) at stations WL (Fig. 1). After calibrating the hydrodynamic model, a validation simulation, keeping the parameters defined previously, was carried out from May to August of 2018, and the results of the model's surface layer were compared with available data. Then, the results of a two-year simulation (with a spin-up period of six months) were used to calibrate (2018) and validate (2019)

the salt, heat transport, and water quality modules. All the simulations were performed with the input conditions described in Section 2.2.

The Root Mean Square Error (*RMSE*), *pBias*, and Pearson Correlation Coefficient (*R*) were determined to quantify the model performance. The *RMSE* evaluates the accuracy of the model results, comparing them with the observed values (Williams and Esteves, 2017). The *pBias* quantifies whether the model is systematically underestimating or overestimating observations (Allen et al., 2007). Negative *pBias* represents a model overestimation, while positive represents an underestimation. According to Allen et al. (2007), the performance levels can be categorized as excellent $|pBias| < 10$ %, very good $10\ \% \leq |pBias| < 20$ %, good $20\ \% \leq |pBias| < 40$ %, and poor $|pBias| \geq 40$ %. Finally, *R* measures the level of correlation between observed data and numerical model results (Williams and Esteves, 2017). *R* was only computed for sea surface height since the data series for the other variables have a short duration.

2.5. Climatic data and scenarios

Two numerical simulations, representing historical (1995–2014) and future (2081–2100) periods, were performed for 12 months (after a spin-up of six months) to anticipate the severest impacts of climate change in the Sado estuary. For the future period, it was considered the most pessimistic greenhouse gas emission scenario (SSP5–8.5) from the 6th Assessment Report of the Intergovernmental Panel on Climate Change (IPCC, 2021), which includes CO_2 emissions tripled by 2075.

In this context, data from the Max Planck Institute for Meteorology climatic model MPI − ESM1.2 (Jungclaus et al., 2013) was used at the ocean's open boundary, which is part of phase 6 of the Coupled Model Intercomparison Project (CMIP), focused on understanding the past, present, and future climate change resulting from natural evolution and anthropogenic pressures. Its selection is motivated by the solid performance in reproducing diverse ocean physical and biochemical properties (Laurent et al., 2021).

Thus, a climatology of the oceanic variables (water temperature, salinity, Chl-*a*, DO, pH, NO_3, PO_4, and NH_4) close to the study area was computed for the historical and future periods, and it was implemented as open boundary conditions. According to climatology, all variables are expected to decrease in the future, except water temperature, which is expected to increase by 10 %. Salinity, Chl-*a*, DO, pH, and nutrients (NO_3, PO_4, and NH_4) will decrease by 2, 10, 3.5, 2.5, and 30 %, respectively. In the future scenario, it was considered a sea level rise of 0.67 m (Lopes et al., 2022).

The atmospheric fields, both for present and future conditions, were obtained from a high-resolution WRF (Weather Research and Forecasting) model simulation over continental Portugal, with 6 km of horizontal resolution, and initial and boundary conditions taken from the same model that supplied the oceanic data, the MPI − ESM1.2 (Carvalho et al., 2021; Marta-Almeida et al., 2016). The average differences of the atmospheric inputs between future and historical periods are +13.5 % in air temperature, +1.5 % in relative humidity, +2.5 % in net radiation, and −1 % in wind speed.

For the future scenario, a 25 % reduction in the river discharge was considered, taking into account the Hydrological Research Unit of the Swedish Meteorological and Hydrological Institute (SMHI, https://hypeweb.smhi.se/) projections by the end of the 21st century regarding the IPCC's highest emission scenario (RCP8.5). Due to data limitations, the concentrations of the water quality properties for historical and future scenarios were considered the same as those used in the calibration and validation simulations.

2.6. Suitability index

In Portugal, IPMA provides information on the current status of the permission/interdiction of bivalve harvesting along the coastal region and in the estuarine systems. Through IPMA's webpage (https://www.ipma.pt/en/bivalves/zonas/), it is possible to check which are the production areas and what species exist there. The Sado estuary has two exploitation zones (ESD1 and ESD2), and the main shellfish species produced there are the European Flat Oyster and the Portuguese Oyster. Since the environmental thresholds for these species are quite similar, in this study, the suitable areas to develop aquaculture activities in the Sado estuary were carried out only for the Portuguese Oyster but, in addition, one of the most important clam species at a national level, the Grooved Carpet Shell (*Ruditapes decussatus*) was also considered. This clam species has a strong economic impact, being extensively exploited in Ria Formosa, another Portuguese coastal system, through several exploitation units. According to IPMA's website, there are some natural banks of *R. decussatus* in the Sado estuary, so the possibility of exploring this clam species becomes very advantageous, depending on the environmental conditions and the places chosen for exploitation.

It is important to mention that clams are harvested differently from oysters (usually by planting clam seed (MMO, 2019)), and the Sado estuary does not present the same characteristics as the Ria Formosa for the exploitation of clams using this method. However, recent studies using an oyster's similar cultivation method (through structures/cages submerged in the water column) have revealed that clams can grow more and avoid predators and potential pathogens compared to growing underground (Ishihi et al., 2017; Lee et al., 2020; Marshall and Dunham, 2013).

The suitable areas to develop aquaculture activities in the Sado estuary were investigated through a Suitability Index (*SI*) computed for seasonal simulations, following Picado et al. (2020) and Vaz et al. (2021) methodologies. This methodology is mainly based on the water column's environmental factors (water temperature, salinity, pH, Chl-*a*, and DO). Therefore, to take a step forward in this study, the spatial constraints (bathymetry, current speeds, presence of protected areas, distance to industries, navigation channels, and Wastewater Treatment Plant (WWTP)) were also considered. These constraints were dissected by Gomes (2019) and are presented in Fig. 1.

For both species, the most important physical and biological factors for a favorable and healthy development are the water depth, the current velocity, the water temperature and salinity, the available Chl-*a*, and the levels of DO and pH. Water temperature and salinity are important physical factors affecting the abundance and distribution of bivalves (Rato et al., 2022). Water temperature influences the metabolism affecting seasonal growth and may be responsible for the difference in bivalve growth (Azeredo et al., 2018; MMO, 2019). Bivalves are euryhaline species that suffer naturally from salinity changes in the environment and are generally tolerant to salinity fluctuations. However, if these variations are too severe, they may cause changes in physiological and behavioral responses and, in acute situations, high mortalities (Rato et al., 2022). In the intertidal areas, with shallower depths and lower velocities, more food is available, leading to higher growth rates and larger sizes of the bivalves species (Azeredo et al., 2018). In addition, the lower levels of DO and pH may affect metabolic processes like food intake, oxygen consumption, and ammonia excretion by some bivalve species (Liu and He, 2012; MMO, 2019; Stevens and Gobler, 2018).

The optimal and minimum/maximum thresholds of each environmental property for both species are listed in Table 1. It is important to mention that nutrients are not included in the index calculation due to the difficulty of establishing threshold and optimal limits for these variables. However,

Table 1
Environmental optimal and thresholds for growth and development of Grooved Carpet Shell and Portuguese Oyster (Azeredo et al., 2018; MMO, 2019; Picado et al., 2020; Rato et al., 2022; https://longline.co.uk/meta/list).

Environmental properties	Grooved carpet shell		Portuguese oyster	
	Threshold	Optimal	Threshold	Optimal
Water temperature (°C)	2–30	18–24	3–35	15–25
Salinity	15–40	25–35	15–40	25–35
DO (mgL^{-1})	2–10	5–8	4–10	5–8
pH	6.5–9.0	7.0–8.5	6.5–9.0	7.5–8.5
Chlorophyll-*a* (μgL^{-1})	> 1	> 2	> 1	> 8
Depth (m)	0–20		0–7	
Current speed (ms^{-1})	0.01–0.35		0.01–0.50	

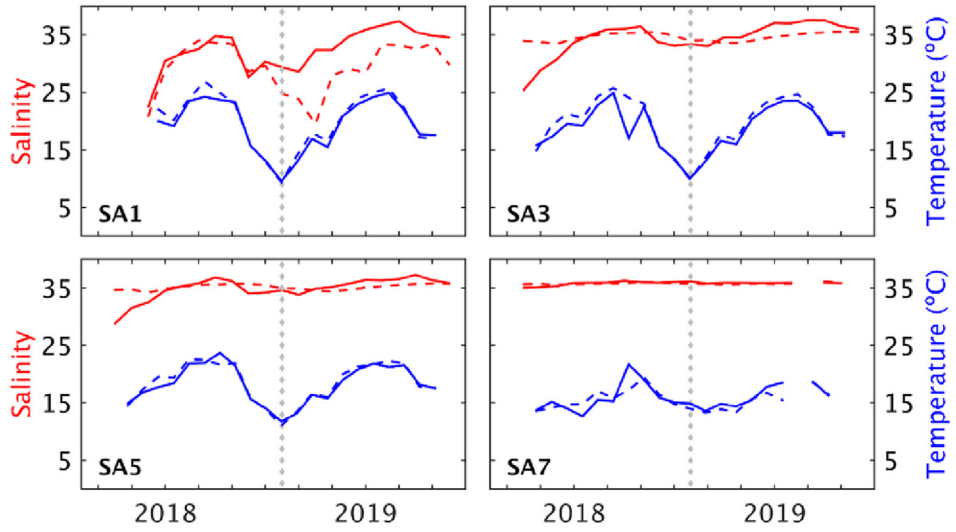

Fig. 2. Annual comparison between observed (solid lines) and simulated (dash lines) salinity and water temperature for stations SA1, SA3, SA5, and SA7. The dashed vertical grey line indicates the year shift.

their importance is indirectly considered since they affect other variables such as Chl-*a* or pH.

Picado et al. (2020) assigned a weight of importance to each of the above environmental properties (except for water depth and current speed) with a pairwise comparison applying the AHP (Analytic Hierarchy Process) method. The AHP method identified the water temperature as the most important factor for bivalve growth, accounting for 38 %, followed by Chl-*a* accessibility (29 %) and water salinity (21 %). With 8 % and 4 %, the DO and pH have the lowest influences, respectively. These authors focused their study on two systems (Minho and Lima estuaries) that have different characteristics (for example, geomorphology and freshwater inflow) compared with the Sado estuary. However, taking into account the species' optimal and threshold limits (Table 1) along with the observed data at the SA stations, it was decided to consider the same variable's weights.

Indeed, as previously stated, water temperature and salinity are two of the most important physical factors affecting the bivalve's energy balance, level of activity, and physiological processes. The availability of phytoplankton biomass is important, as microalgae can represent the major food source for filter-feeder organisms. The combined effects of water temperature and primary production can explain up to 85 % of growth performance differences between bivalve farms (MMO, 2019). The DO concentration in water is influenced by many factors, such as water temperature, salinity, and biological activity (photosynthesis and respiration) (MMO, 2019). At increased temperatures, oxygen availability decreases as the amount of oxygen dissolved in the water reduces. Also, at higher salinities, the DO decreases. Ocean water (typically with high salinities) has 20 % less DO than freshwater with salinity zero, at the same temperature (Truesdale et al., 1955). pH is an important water property, and its reduction (acidification) is potentially harmful to aquatic organisms. However, compared to the other properties, pH is more constant throughout the system and has less impact on the growth of bivalves (larval) than the water temperature and salinity (Thiyagarajan and Ko, 2012). This dependency on other factors reduces the importance weight of DO and pH.

After the weight assignment, a score between 0 and 5 was attributed to each water property, combining the environmental thresholds for each specie and the numerical results of historical and future simulations. Then, the

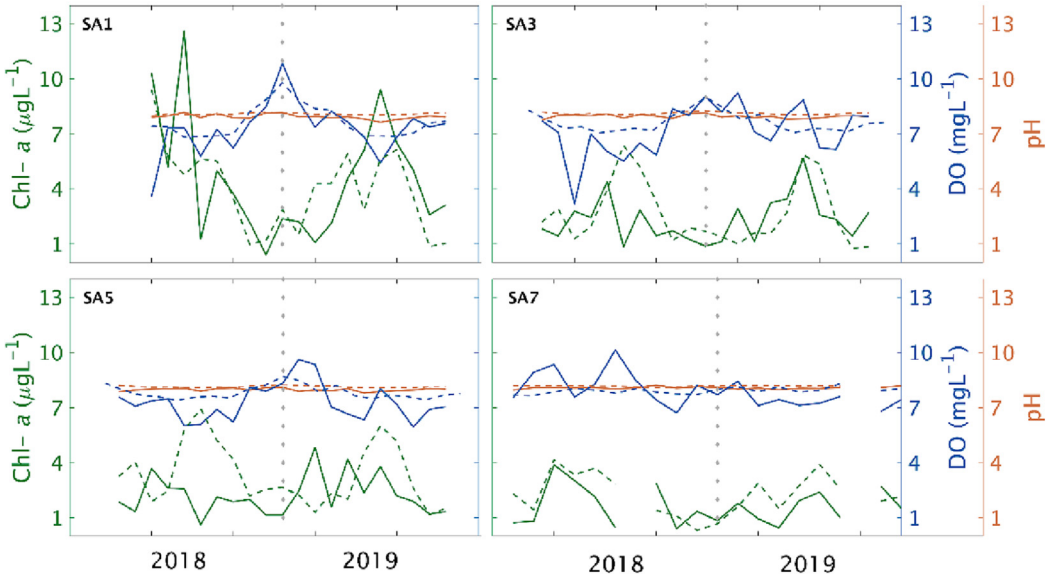

Fig. 3. Annual comparison between observed and simulated Chl-*a*, DO, and pH at stations SA1, SA3, SA5, and SA7. The solid lines represent the in-situ data, and the dashed lines show the model results. The year 2018 corresponds to the calibration period, and the year 2019 to the validation period.

SI was computed as the weighted geometric mean of the scored environmental factors as described in the following equation:

$$SI = \left(\prod_{i=1}^{n} x_i^{w_i}\right)^{\frac{1}{\sum_{i=1}^{n} w_i}} \wedge SI = 0 \text{ if } Z_j < Z_{min} \wedge SI = 0 \text{ if } Z_j > Z_{max}$$

where x_i is the scored environmental factors, w_i the weights and n the number of each variable defined in the AHP (water temperature, salinity, DO, pH, and Chl-*a* concentration), and Z_j corresponds to the depth and current speed thresholds. When Z_j is out of the thresholds, a score of 0 is considered. As mentioned, based on the outcomes of Gomes (2019), spatial constraints such as maritime navigation channels, industrial zones, environmental zones with protected areas, and salt marshes were identified as unsuitable regions.

Finally, the suitability for aquaculture development in the Sado estuary was defined in five classes: Unsuitable [0–1], Poorly Suitable [1–2], Moderately Suitable [2–3], Suitable [3–4], and Highly Suitable [4–5].

3. Results

3.1. Evaluation of the model's accuracy

3.1.1. Water level

Predicted sea surface height was compared with harmonic tide reconstructions for the station's WL presented in Fig. 1. The year 2010 was used for calibration procedures, and 2018 for validation. Generally, an excellent agreement for amplitude and phase between data and model results is observed (Fig. SM2), with *RMSE* ranging from 5 to 8 cm for calibration and validation periods. The *pBias* indicate that the model frequently overestimates the water level amplitudes but with minimal differences. The highest *pBias* (1.57 %) was found in station WL5. Finally, in all stations, *R* exceeds 0.99 with a significance level >95 %, confirming that the model results and observations have an excellent positive correlation.

3.1.2. Salinity and water temperature

The water temperature and salinity data presented in Section 2.3 were used to calibrate and validate the model's salt and heat transport module. The year 2018 was used for calibration, and the year 2019 for validation of the model's accuracy. Water temperature and salinity data are available for a total of 7 stations, and the statistical errors obtained for each station are presented in Table SM2. For salinity, the upstream station (SA1) has the maximum *RMSE* (3.61 and 5.61), while station SA7 (more downstream) presents the minimum *RMSE* (0.31 and 0.19) for calibration and validation periods, respectively. Model results in all locations overestimate the salinity data during 2018 and underestimate it during 2019. Regarding water temperature, SA5 presents the lowest *RMSE* in 2018 (0.91 °C) and 2019 (0.52 °C), whereas SA4 has the highest *RMSE* in 2018 (2.53 °C) and SA7 in 2019 (1.05 °C).

In addition, Fig. 2 displays the results for stations SA1, SA3, SA5, and SA7 since their location covers the whole estuary. The available data preclude comparison at the tidal timescale, only allowing the identification of seasonal patterns.

A typical seasonal and longitudinal pattern of subtropical regions is identified with higher water temperatures upstream in summer (near 25 °C) and lower in winter (around 10 °C). This physical property is highly represented in all locations for both years, with lower *RMSE* and *pBias* (Table SM2) for the validation year (2019).

Regarding salinity, there is a small seasonal pattern at the stations closer to the Sado River, with a slight decrease during the winter months. In the downstream station (SA7), this pattern is inexistent. The comparison between the model results and observations shows higher differences in station SA1 (particularly in 2019) and minor differences in the remaining stations, especially downstream (Table SM2). The salinity mismatches between the two years can be related to the climatology of river flow data, which substantially impacts the reproduction of the system dynamics.

To calibrate and validate the water temperature and salinity model results through the water column, available vertical profiles of these properties at stations SA6, SA7, and SA8 were compared with model results, and the respective errors were quantified (Fig. SM3 and Table SM3). In Fig. SM3, the displayed profiles cover different months, and Table SM3 quantifies the comparison errors for all the available data. Visually, the excellent capacity of this model configuration to reproduce the vertical homogeneity of the estuary is noticeable.

Also, the good results presented in Fig. SM3 are corroborated numerically by averaging the results in Table SM3 for the three stations (SA6, SA7, and SA8). For 2018, the water temperature presents an average *RMSE* of 0.52 °C and |*pBias*| of 2.91 %. For salinity, the average statistical errors were *RMSE* of 0.08 and a very small |*pBias*| of 0.28 %. The results are similar for the validation period (2019), with average *RMSE* of 0.68 °C and 0.20 and |*pBias*| of 4.68 % and 0.59 % for the water temperature and salinity, respectively.

3.1.3. Water quality

The water quality module was calibrated and validated using the data from the campaigns quoted in Section 2.3. The comparison between observations of Chl-*a*, DO, pH, NO_3, PO_4, and NH_4 and model results show a good agreement, with some differences throughout the estuary (Fig. 3 and Tables SM4 and SM5). The upstream stations present a different pattern from the downstream ones. Fig. 3 demonstrates the efficiency of the WAQ model in reproducing the annual patterns and concentration magnitudes of Chl-*a*, which show a longitudinal gradient along the Sado estuary, with lower concentrations near the mouth (SA7) and higher concentrations upstream (SA1). The model developed reveals its ability to represent this pattern, presenting the best results at station SA6 and the poorest at SA1 (Table SM4).

WAQ model overestimates the pH at all stations with a small *RMSE* (ranging between 0.12 and 0.21), as presented in Table SM4. Regarding DO, the highest *RMSE* is approx. 1.60 mgL^{-1} at SA3 and SA4 in 2018 with a *pBias* of −16.55 % and −18.99 %, respectively. An overestimation of this variable is also observed in most of the locations under analysis. In general, the performance obtained for the model validation is slightly better than for the calibration.

Regarding nutrients, the best results were obtained for NO_3 and the poorest for NH_4 (Table SM5). For the calibration year, the lowest *RMSE* and *pBias* for the three nutrients are found at SA7 and the highest near SA1. As for Chl-*a*, DO, and pH variables, an overestimation of the nutrients is observed in most of the stations. Also, the model performed better during the validation than during the calibration period.

Despite the lack of vertical water quality in situ data available to calibrate and validate the vertical structure of the variables under analysis, as the system was found to be mostly vertically homogeneous, it can be considered that the model can adequately reproduce the in-depth nutrient variation since it accurately represents the water quality variables observed at a single level.

3.2. Climate change simulations

3.2.1. Vertical and longitudinal variation of water properties

The most critical water properties identified in Section 2.6 for the bivalve species exploitation were analyzed to assess the possible impact of climate change on the aquaculture activity at the Sado estuary.

The vertical distribution of salinity, water temperature, Chl-*a*, DO, and pH along the longitudinal transects A and B (Fig. 1) during dry and wet seasons are presented in Figs. SM4, SM5, SM6, and SM7. These transects exhibit a vertical homogeneity during both summer and winter, supporting the vertical results presented in the calibration and validation section, and therefore, the analysis will be focused on the longitudinal variations.

Historical (1995–2014) horizontal maps of average water temperature, salinity, Chl-*a*, DO, and pH during a wet period (winter months – January, February, and March) and a dry period (summer months – July, August, and September) are presented in Fig. 4. During the wet period, on average,

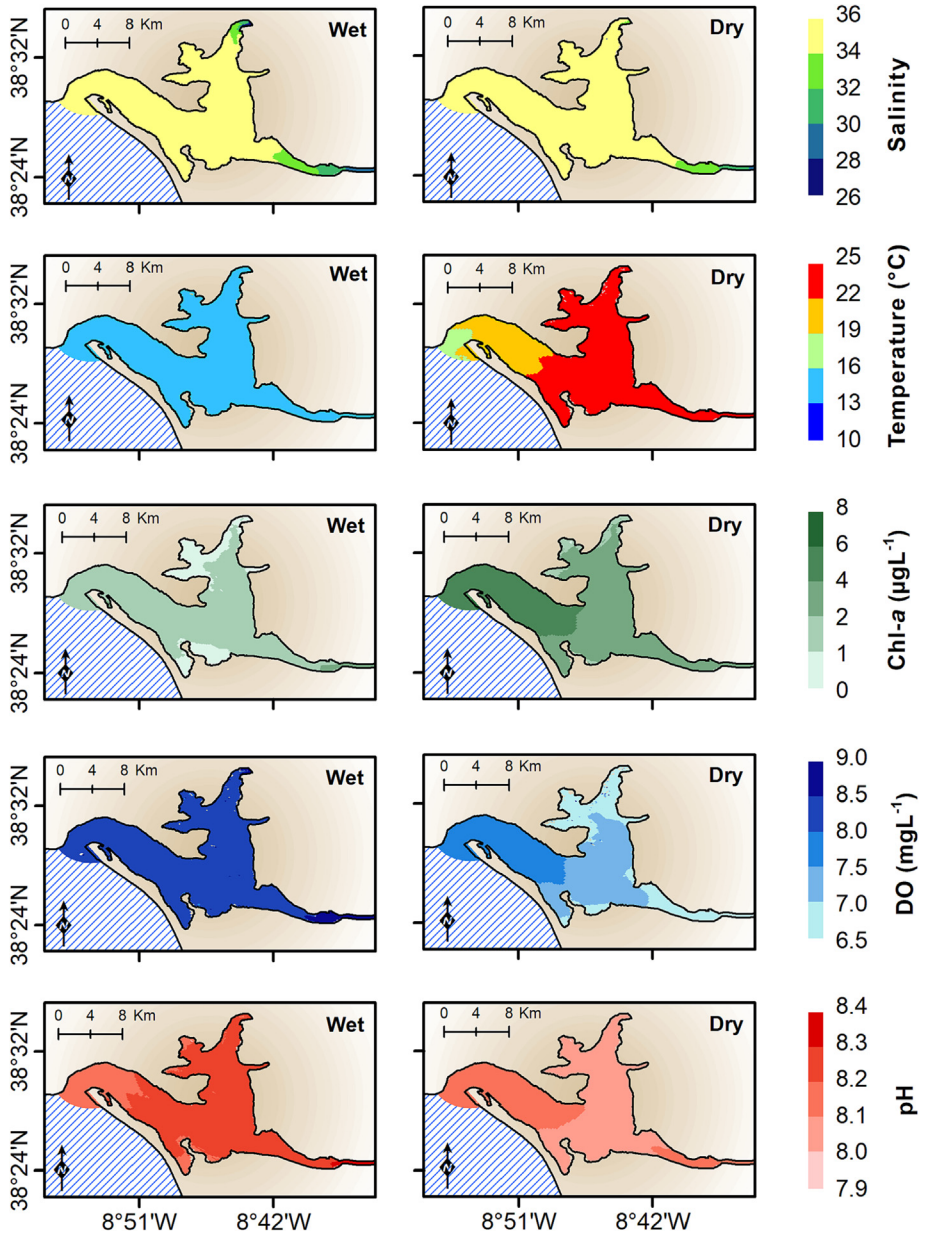

Fig. 4. Historical maps of the average salinity, water temperature, Chl-*a* and DO concentrations, and pH for the wet and dry seasons.

salinity ranges from 26 near the tributaries to 36 in the estuary mouth and central region, while the water temperature presents a small variation, between 13 and 14 °C, throughout the estuary (Figs. 4, SM5, and SM6). Regarding the Chl-*a* and DO, the highest concentrations were found near the main freshwater source (approximately 2 μgL^{-1} for Chl-*a* and between 8.5 and 9 mgL^{-1} for DO). Despite small pH variations throughout the estuary, a longitudinal gradient is observed, with values between 8.1 in the estuary mouth and 8.3 upstream.

During the summer months, the estuary presents a typical temperate estuarine distribution with a decrease in salinity (from ~35 to 30) and an increase in water temperature (16 to 25 °C) upstream (Figs. 4, SM3, and SM4). The model predicts an increase in the central and upstream regions up to 8 μgL^{-1} of Chl-*a*. During this season, the estuary also turns less oxygenated (6.5–7 mgL^{-1}), and the pH (approx. 8) slightly reduces in the central and upstream areas, compared to the wet season.

To understand the implications of climate changes in the estuary's main properties, an analysis of the longitudinal differences between the future (2081–2100) and historical (1995–2014) scenarios was performed and is presented in Fig. 5. During the wet season, a slight decrease in salinity (between 0 and 1) is projected. However, an increase in the salt content, up to 4, is predicted at the Alcácer channel. An increase in water temperature (up to 2 °C) is also expected in the future. The Chl-*a* increases (up to 2 μgL^{-1}) in most of the estuary, except for the Alcácer channel, where a decrease is observed. The DO and pH are expected to decrease (-0.5 mgL^{-1} and -0.05) in the whole system (Fig. 5).

During the dry season, model projections suggest a small salinity decrease in the central region and an increase near the main freshwater source. Also, an average increase of approximately 1.5 °C in the water temperature and, consequently, a decrease in DO concentration (approximately -0.3 mgL^{-1}) are predicted for the future in the whole estuary. Chl-*a* results suggest an average increase of nearly 1 μgL^{-1}, with the central region reaching 3–4 μgL^{-1}, whereas no changes in pH are expected during summer.

3.2.2. Suitability index maps

Suitability Index maps (Figs. 6 and 7), based on the previously described environmental factors and spatial constraints, are presented to assess the aquaculture production potential and identify the most suitable areas for

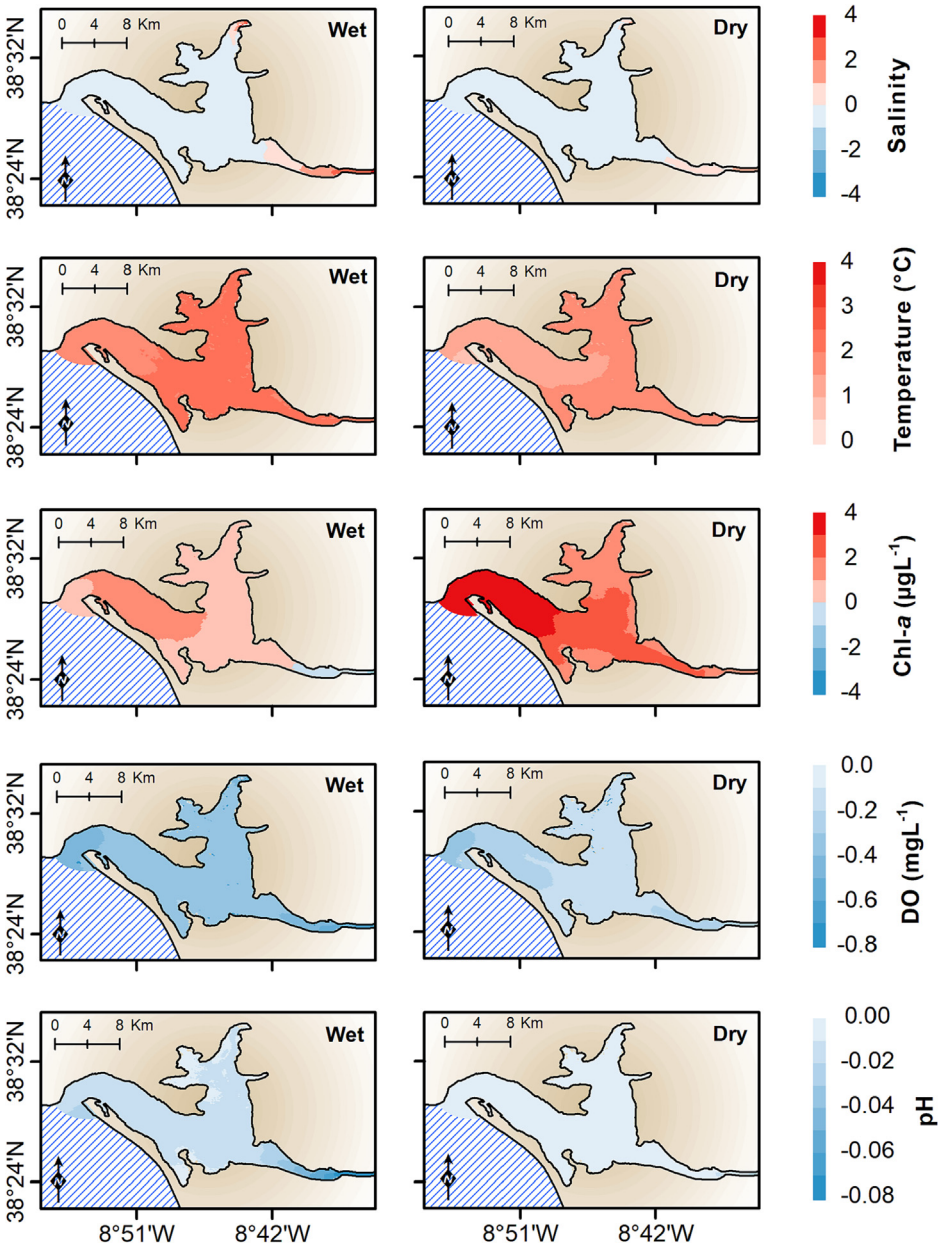

Fig. 5. Differences between future and historical periods for the salinity, water temperature, Chl-*a* and DO concentrations, and pH during the wet and dry seasons.

the development of this activity for historical and future scenarios. Most of the estuary is considered Unsuitable for aquaculture production mainly due to bathymetric and spatial constraints, like Environmental Protected Areas (EPA), navigation channels that give access to ports, and proximity to possible industries and WWTP effluents. These spatial constraints were assumed to remain unchanged in the future.

During the wet season (Fig. 6), for the historical period, model results suggest that the upstream north part of the estuary (near Marateca) presents moderately suitable conditions for the production of Grooved Carpet Shell and poorly suitable conditions for the Portuguese Oyster exploitation. In the future, aquaculture exploitation conditions are expected to improve for both species due to the changes in environmental factors. Indeed, the Marateca region shows highly suitable conditions for Grooved Carpet Shell production and moderately suitable conditions for the Portuguese Oyster (Fig. 6).

Considering the dry season (Fig. 7), the historical SI map suggests highly suitable conditions for the Grooved Carpet Shell exploitation and, for the Portuguese Oyster, suitable and moderately suitable conditions. In the future, it is observed an improvement in the environmental conditions, mainly for the oyster, compared to the wet season. As a result, the suitability index in the upstream areas changes from moderately suitable to suitable.

Since the system is vertically homogeneous and the Suitability Index derives from the environmental factors, it is assumed that the SI in-depth has the same pattern as the horizontal maps and, consequently, will not be exhibited.

4. Discussion

4.1. Modeling performance

The numerical model Delft3D was implemented for the Sado estuary in 3D mode. Results showed that the model is robust and accurately reproduces the data. Indeed, the average *RMSE* for the sea surface height was 7 cm, representing an excellent agreement between the model and the data (Dias et al., 2000), with the highest errors in the upstream stations.

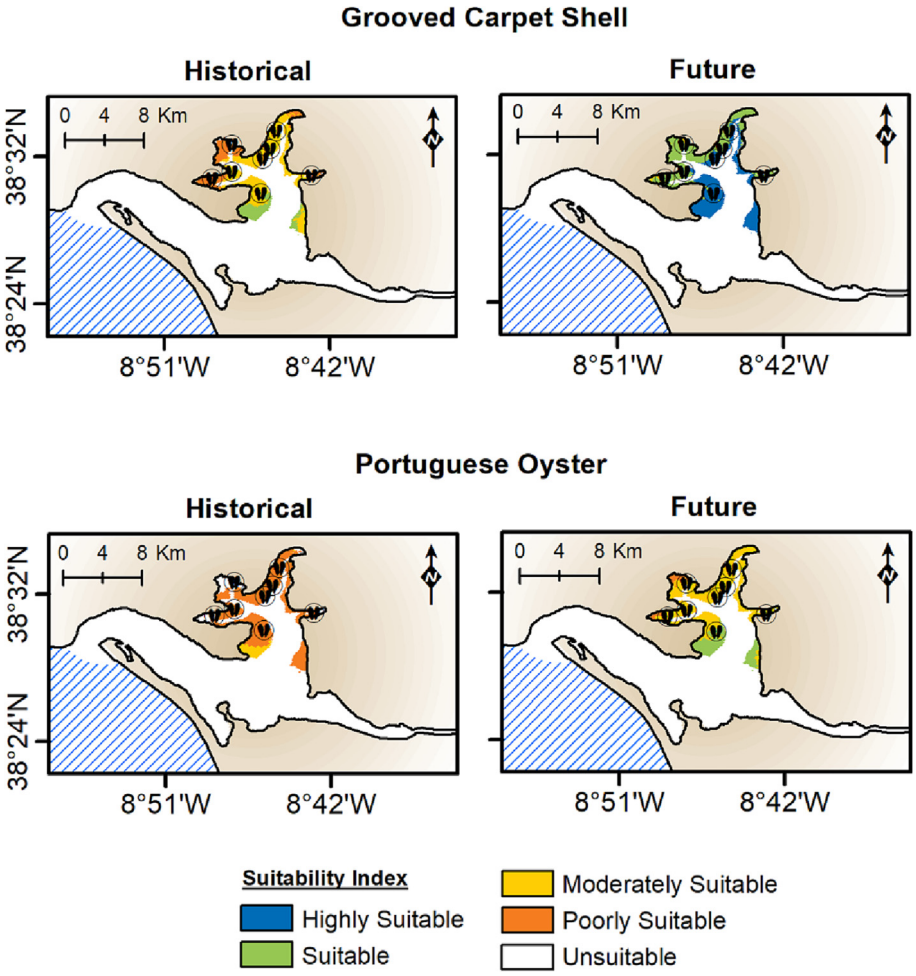

Fig. 6. Suitability Index maps for the Grooved Carpet Shell and Portuguese Oyster aquaculture developments at the Sado estuary during the wet season for historical (left panel) and future (right panel) periods. The shellfish farms locations are also shown.

The errors appear to be mainly due to uncertainties in bathymetric data. Notwithstanding, similar results were obtained in previous modeling studies in the Sado estuary (Maretec, 2002; Ribeiro et al., 2016) and in other similar systems (Dias et al., 2021; Lopes et al., 2022).

The water temperature and salinity results along the estuary were very good and concordant with other studies (Martins et al., 2002; Ribeiro et al., 2016). However, the model's capacity to represent the salinity variations along the estuary decreases moving upstream, as shown in Fig. 2 and Table SM2. The poorest result was achieved at station SA1, with an *RMSE* of 3.61 and 5.61 for 2018 and 2019, respectively. These areas are generally more susceptible to changes in the volume of freshwater introduced into the system, so the existing limitations in the field data used to force the model in the open river boundary imply a lower quality of the model results in these regions. In contrast, the results at station SA7 are excellent, with *RMSE* of 0.31 and 0.19 and *pBias* of −0.05 % and 0.39 % for 2018 and 2019, respectively.

Considering the water temperature, a consistent *RMSE* is found throughout the system. However, for the calibration period (2018), the *RMSE* is high at stations SA3 and SA4 (2.28 °C and 2.53 °C, respectively). This result is mainly a direct consequence of the difference between the observed (approx. 17 °C) and simulated (approx. 24 °C) water temperature in September (Fig. 2). Considering the patterns of observed and simulated water temperatures along the year for all stations, the values in September for these two stations look to be outliers difficult to justify. Thus, it is hypothesized that a sporadic event or error in the measurement might have justified these abnormal values. Moreover, if we assume that these two observations are outliers and remove them from the *RMSE* computation, the error would decrease to 1.04 °C (SA3) and 1.02 °C (SA4), and the corresponding *pBias* would also decrease to −4.13 % and −4.82 % respectively.

Nevertheless, it is also verified an improvement in the results between the calibration and validation periods, which suggests that the climatology adopted may be more consistent with the conditions of the validation period than with those of the calibration period. Vertically, the estuary can be classified as homogeneous, which is in line with previous studies (Biguino et al., 2021; Ferreira et al., 2005), and Fig. SM3 exhibits the Delft3D model's efficiency in representing the vertical structure of water temperature and salinity.

Concerning the water quality modeling process, analyses conducted in previous studies (Arhonditsis and Brett, 2004; Dynamic Solutions, LLC, 2013) concluded that DO typically has the lowest error value, followed by nutrients and phytoplankton, with respective *RMSE*s of 20 % for DO, 50 % for nutrient and suspended solids, and 100 % for algae biomass. In this study, the results for DO and pH are very good since they showed low *RMSE* and *pBias*. For Chl-*a*, the results are not as good as for DO and pH, with an average *RMSE* (1.9 μgL^{-1}) and *pBias* (38 %). In a study carried out in the North Sea, Zijl et al. (2021) reported RMSE between 1 and 12 μgL^{-1} for Chl-*a*, which are larger than those presented here.

Despite the higher *RMSE* and *pBias* obtained for the water quality variables compared with those obtained for the physical variables (water level, salinity, and water temperature), these results are in line with other publications (Fraysse et al., 2013; Mendes et al., 2021; Rodrigues et al., 2021; Wang et al., 2017; Zijl et al., 2021). The water quality modeling performance is recognized to decrease from the hydrodynamics and heat and salt transport models, mostly due to the high complexity of all the

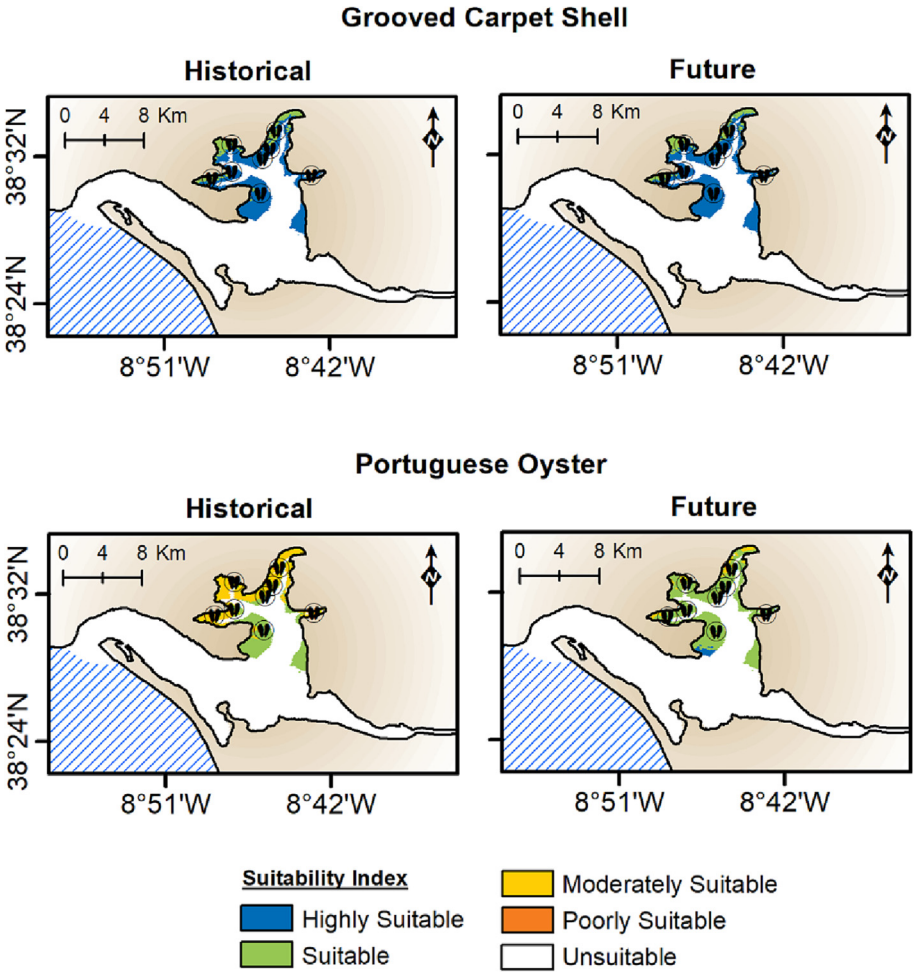

Fig. 7. Suitability Index maps for the Grooved Carpet Shell and Portuguese Oyster aquaculture developments at the Sado estuary during the dry season for historical (left panel) and future (right panel) periods. The shellfish farms locations are also shown.

biological and chemical processes and to the successive approximations and parametrizations used in these models (Allen et al., 2007; Vaz et al., 2019). Also, nutrient unpredictability and the lack of good load data are important limitations in water quality modeling (Mateus et al., 2012; Vaz et al., 2015).

Collecting in situ physical and biogeochemical continuous data (both spatial and vertical) is of utmost importance to address these limitations and enhance the model's performance. Increasing the grid resolution and updating the bathymetry (with recent data) may improve the model performance. Furthermore, incorporating additional processes into the water quality model, such as diffusive exchanges at the sediment-water interface, may also be beneficial (Rodrigues et al., 2021; Wang et al., 2017; Zijl et al., 2021).

4.2. Climate change effects on environmental properties

The Sado estuary, throughout the historical period, presents different spatial gradients between each season for the environmental properties. During winter, a downstream-upstream gradient is present for salinity (Fig. 4) as a consequence of increased rainfall and river discharge typical of this season. A homogeneity throughout the estuary is found regarding water temperature, Chl-*a*, and pH. These results align with other studies in similar locations (de Pablo et al., 2022; Ferreira et al., 2003).

The highest DO concentrations were observed during winter when the water temperature was lower. In fact, DO solubility is directly related to the water temperature, increasing when temperature decreases and vice versa, and might also cause the reduction of DO during summer. In another Portuguese coastal system (Ria Formosa), Cravo et al. (2020) captured these same opposite patterns in their field data, indicating that the water quality model used in this study can reliably represent DO seasonal patterns.

During the dry season, the water temperature is higher than in winter due to the higher intensity of solar radiation. The average salinity in the estuary rises to 35, revealing the impact of lower fluvial inputs, higher evaporation, and the incoming salt water from the Atlantic Ocean. Furthermore, the low fluvial discharge dissipates the slight longitudinal salinity gradient observed in the wet season. The highest concentrations of Chl-*a* were observed during the dry period and in the central part of the estuary since physicochemical parameters, such as water temperature, contribute directly to its growth (Brito et al., 2023; Masson and Peña, 2009). The pH is homogenous in the entire system ranging between 8 and 8.2.

The differences between historical and future maps presented in Fig. 5 revealed the impact of the predicted modifications of oceanic (e.g., sea level rise, salinity decrease, or water temperature increase), riverine (e.g., a decrease of fluvial discharge), and atmospheric (e.g., air temperature increase) drivers imposed in the Sado estuary boundaries in a climate change context. Since the estuarine water strongly depends on ocean water, these changes will be reflected along the estuary.

As shown in Fig. 5, due to an increase of 10 % in ocean water temperature, 13.5 % in air temperature, and 10 % in net solar radiation, model results forecast an increase between 1.5 and 2 °C in water temperature and, consequently, an increase between 2 and 4 μgL^{-1} in the Chl-*a* concentration and a decrease between 0.3 and 0.5 mgL^{-1} in DO. An increase in Chl-*a* concentration is expected to be associated with an increase in DO

since photosynthesis produces oxygen. However, this increase in Chl-*a* may not be directly related to the increase in photosynthetic activity since the photosynthetic process depends on more factors, such as light, carbon dioxide (CO_2), and water temperature. Therefore, the results presented in Fig. 5 lead us to believe that the reduction of DO could be even more significant if there were no increase in the Ch-*a* concentration or that the impact of the increase in water temperature is more substantial than an increase in the Chl-*a* concentration.

A 2 % decrease in ocean salinity and a sea level rise of 0.67 m are expected to cause a slight reduction in salinity (between 0 and 1) in the lower and central regions of the estuary. However, an increase in salinity is anticipated in the influence zone of the tributaries. This increase can be attributed to the joint effect of the increase in tidal prism induced by the sea level rise and the reduction in river flow by 25 %, which has more influence mainly during the wet season. Also, due to river flow reduction, a decrease of up to 1 μgL^{-1} in Chl-*a* and up to 0.07 in pH is foreseen at the Alcácer channel during the wet season.

4.3. Suitability index potential and aquaculture prospect

This study intends to contribute to the identification of the most suitable regions for aquaculture production in the Sado estuary, considering the methodologies presented by Gomes (2019), Picado et al. (2020), and Vaz et al. (2021). These regions were defined through the computation of a SI for two bivalve species for historical and future conditions during wet and dry seasons, considering the estuary's water quality and spatial constraints. The SI was calculated for two bivalve species, the Grooved Carpet Shell and the Portuguese Oyster.

Despite the favorable environmental conditions, approximately 80 % of the total area of the estuary is considered unsuitable (Gomes, 2019) due to the spatial constraints mentioned in Section 2.6. In addition to the regions excluded by the bathymetric restriction near Comporta, the intertidal plains are also unsuitable due to EPAs, salt marshes, and boat transportation routes. Along the Tróia sand bar, the presence of navigation terminals also makes this area unsuitable. In the central region, near the SA2 station, another protected area precludes the implementation of aquaculture sites due to its high ecological sensitivity. Finally, in the north part of the estuary, from the estuary's mouth to the Lisnave shipyard (near SA5 station), the industries and the WWTP location turn this entire region unsuitable. This industry belt, with a high concentration of heavy industries (Caeiro et al., 2005; Carreira et al., 2013), is characterized by potential polluting activities, and the WWTP effluents, which even treated may contain excessive nutrient loads that could jeopardize the eventual shellfish farms in the area.

By considering these spatial constraints in the SI, we can minimize potential negative impacts on the aquacultures or the surrounding ecosystem. For example, if a proposed aquaculture site is located in a protected area or a navigation channel, it could disrupt the natural habitat of various marine species or interfere with shipping routes, causing negative economic and environmental impacts. Thus, the suitable aquaculture areas are restricted to the upper part of the estuary (Figs. 6 and 7), following the current locations of established infrastructures. (https://webgis.dgrm.mm.gov.pt/portal/apps/webappviewer/index.html?id=9bc91b21cc8b420ba784829970cb5059).

Regarding the historical period, during winter (Fig. 6), model results suggest that the upstream north part of the estuary (near Marateca) is moderately suitable for the Grooved Carpet Shell production, while for the Portuguese Oyster, the region is mostly poorly suitable. These findings are related to the bivalves' sensitivity to low water temperatures (<18 °C for the Grooved Carpet Shell and <15 °C for the Portuguese Oyster) and to the availability of Chl-*a* in the surrounding environment. During the dry season, the water temperature and salinity values are typically higher than for the wet season (Fig. 4), ranging from 19 to 25 °C and 34 to 36 in the center of the estuary, respectively. These ranges are within the optimal thresholds for the considered bivalve species, and therefore, the suitability for these species' production in summer is higher than in winter.

Assessing the other environmental factors (DO and Chl-*a* concentration and pH), the mean values for both seasons are in the range of the optimal thresholds and are not considered critical for the suitability of bivalves' exploitation in the Sado estuary. However, as shown in Fig. 3, the model fairly reproduces the DO observations, not reaching its minimum (around 4 mgL^{-1}) captured in May at the upstream stations. These events are difficult to predict due to their local origin and might be related to punctual episodes of sewage discharges that are not considered in the model implementation or might depend on organic matter accumulation during specific periods that can contribute to a decrease in the DO (for example during night periods). Furthermore, it should be noted that while the DO dataset spans a period of one year, the measurements were taken only once a month, which may introduce some uncertainties as daily variations are not accounted for. DO has a significant daily fluctuation (Nascimento et al., 2021), with minimal concentrations observed in the early morning due to overnight respiration (Cravo et al., 2020), which may affect the bivalves' development. However, bivalves can tolerate extended periods of hypoxia and anoxia since they are able to maintain respiration rates independent of declining oxygen (Sobral, 1995), yet other factors, such as water temperature or salinity, may affect this tolerance.

Also, according to a recent study about this estuary (Brito et al., 2023), the increase in oyster production resulted in substantial reductions in Chl-*a* availability, associated with increased nutrient concentrations and lower levels of DO, which may negatively affect the suitability of the estuary. Indeed, an increase in the bivalve's biomass leads to a decrease in Chl-*a* and DO since these organisms consume phytoplankton for feeding and oxygen for respiration. As the phytoplankton community declines, oxygen production through photosynthesis decreases, reducing oxygen availability in the water column. Otherwise, nutrient availability increases due to reduced consumption of nutrients by the phytoplankton. Moreover, the predicted increase in water temperature and Chl-*a* concentration from the wet to the dry season is translated into an improvement in the suitability of the north part of the estuary for both species (moderately to highly suitable for the Grooved Carpet Shell and poorly suitable to moderately and suitable for the Portuguese Oyster) as shown in Figs. 6 and 7.

Recent works studied the suitability of different estuarine systems for bivalves and fish development, achieving different conclusions according to the characteristics of each system. For instance, Picado et al. (2020) concluded that the upper regions of Minho and Lima estuaries are not prone to aquaculture development due to the significant fluvial source proximity. According to these authors, the growth of bivalves could be affected by exposition to low salinity during long periods. In the case of the Sado estuary, the low salinity is not a determinant factor since the mean annual discharge of Marateca Creek is negligible and exceptionally reaches 12 m^3s^{-1} (Psuty and Moreira, 2000). Usually, the average salinity in the estuary is above 30. Vaz et al. (2021) concluded that bivalve aquaculture in Ria de Aveiro is mainly limited by local geomorphology and hydrodynamic characteristics, and that Rías Baixas generally show very good conditions except near the margins.

Lastly, the climate change impact on the aquaculture regions' suitability was also assessed. For the wet period (Fig. 6), the increase in Chl-*a* concentration of ~1 μgL^{-1} in the farm areas of the estuary (Fig. 5) becomes the most predominant factor in the improvement of the suitability for bivalve aquaculture. For the dry season (Fig. 7), the suitability of the estuary for Grooved Carpet Sell production remains Highly Suitable. However, if the increase in water temperature is more extensive than projected by climate models, it could have a negative impact on the metabolism of these animals. The metabolism regulation of poikilothermic organisms like bivalves is strongly influenced by biochemical and physiological processes that are directly related to the temperature of the surrounding environment (Filgueira et al., 2016; Woods et al., 2003). Consequently, an increase in the habitat temperature in which these organisms develop can affect their weight and length, affecting their overall growth (Ferreira et al., 2007).

Regarding the Portuguese Oyster, the future changes predicted by the model (increase of water temperature and Chl-*a* concentration) lead to an improvement in the Suitable Index during the wet and dry seasons. In the first, the system classification evolves from poorly to moderately suitable and suitable, and for summer, the upper region from moderately suitable

to suitable. A recent investigation conducted in Rías Baixas concluded that, in the future, the increase in water temperature might favor the settlement of the Pacific Oyster (Des et al., 2022). However, the different characteristics of both systems and the methodologies applied to compute the suitability maps should be considered. Authors considered that favorable conditions for the presence of this oyster occur when the daily mean water temperature is above 18 °C for at least 15 consecutive days. This approach differs from the one presented in this study for the Sado estuary, which considers an optimal water temperature range (15–25 °C) and other variables in the SI calculus. Also, Rías Baixas present an average surface water temperature lower than the Sado estuary, impacting the region's suitability.

5. Conclusions

The study of the possible effects of climate change on aquaculture through a 3D water quality model implementation was achieved. In addition, an analysis of the most important water properties for the growth and welfare of two commercially important bivalve species in the Sado estuary during winter and summer was conducted. This analysis allowed the definition of five suitability classes for aquaculture exploration, leading to mapping the best sites for installing and expanding these infrastructures.

Despite some inconsistencies between model results and field data, a good qualitative and quantitative agreement was accomplished. For future applications, it is crucial to perform in situ measurements mainly in what concerns the tributaries flow and water properties, as well as measurements of nutrients, Chl-*a*, and DO concentrations along the estuary during long periods and with a higher temporal resolution. This new data will be very important to increase the model's accuracy in reproducing the local processes. Moreover, some errors could be minimized if updated bathymetric data is used.

Model results lead to the conclusion that the best locations for aquaculture exploitation are in the northern region of the estuary. During both periods, an improvement in the Suitability Index is observed for future scenarios. These results can be related to the expected increase in water temperature, which contributes positively to Chl-*a* availability.

This work can be replicated for similar coastal systems and possibly be used to encourage the new shellfish production facilities to be implemented in the most suitable locations, providing a real and significant contribution to management plans and maritime spatial planning.

CRediT authorship contribution statement

HPereira: conceptualization, methodology, software, validation, formal analysis, original draft. **APicado:** conceptualization, methodology, software, validation, original draft. **MCSousa:** validation, review & editing. **ACBrito:** in-situ sampling, review & editing. **BBiguino:** in-situ sampling, review & editing. **DCarvalho:** software, review & editing. **JMDias:** resources, review & editing, supervision, project administration.

Data availability

Data will be made available on request.

Declaration of competing interest

The authors declare that they have no known competing financial interests or personal relationships that could have appeared to influence the work reported in this paper.

Acknowledgments

The first author was funded by the Portuguese Foundation for Science and Technology (FCT), with grant number SFRH/BD/138755/2018. Ana C. Brito was funded by FCT through the Scientific Employment Stimulus Programme (CEECIND/00095/2017). Beatriz Biguino was supported by the doctoral grant PRT/BD/152829/2021, funded by the FCT under the MIT Portugal Program. David Carvalho acknowledges FCT for his researcher contract (CEECIND/00563/2020). We acknowledge financial support to CESAM by FCT/MCTES (UIDP/50017/2020 + UIDB/50017/2020 + LA/P/0094/2020) through national funds. This study also had the support of FCT through the strategic project UIDB/04292/2020, awarded to MARE, and through project LA/0069/2020, granted to the Associate Laboratory ARNET. This study was partially supported by the project AQUASADO - Promoting Sustainable Aquaculture in the Sado Estuary (MAR-02.01.91-FEAMP-0051), funded by the Operational Program MAR2020. The work also benefits from the infrastructure CoastNet (PINFRA/22128/2016).

Appendix A. Supplementary data

Supplementary data to this article can be found online at https://doi.org/10.1016/j.scitotenv.2023.164250.

References

Aguiar, M., Sousa, J.B., Dias, J.M., Silva, J.E., Ribeiro, A.S., Mendes, R., 2020. The value function as a decision support tool in unmanned vehicle operations. IFAC-PapersOnLine 53, 14608–14613. https://doi.org/10.1016/j.ifacol.2020.12.1469.

Allen, J.I., Holt, J.T., Blackford, J., Proctor, R., 2007. Error quantification of a high-resolution coupled hydrodynamic-ecosystem coastal-ocean model: part 2. Chlorophyll-a, nutrients and SPM. J. Mar. Syst. 68, 381–404. https://doi.org/10.1016/j.jmarsys.2007.01.005.

Arhonditsis, G., Brett, M., 2004. Evaluation of the current state of mechanistic aquatic biogeochemical modeling. Mar. Ecol. Prog. Ser. 271, 13–26. https://doi.org/10.3354/meps271013.

Azeredo, F.F., Gonçalves, J.F., Hinzmann, M., Vaz-Pires, P., 2018. Manual de cultivo de ostras em Portugal e o código de boas práticas. Instituto de Ciências Biomédicas Abel Salazar - Universidade do Porto, Centro Interdisciplinar de Investigação Marinha e Ambiental, 1st edition.

Barange, M., Merino, G., Blanchard, J.L., Scholtens, J., Harle, J., Allison, E.H., Allen, J.I., Holt, J., Jennings, S., 2014. Impacts of climate change on marine ecosystem production in societies dependent on fisheries. Nat. Clim. Chang. 4, 211–216. https://doi.org/10.1038/nclimate2119.

Bettencourt, A., Ramos, L., 2003. Estuários Portugueses. Instituto da Água, Lisboa.

Biguino, B., Sousa, F., Brito, A.C., 2021. Variability of currents and water column structure in a temperate estuarine system (Sado Estuary), Portugal. Water 13, 187. https://doi.org/10.3390/w13020187.

Biguino, B., Haigh, I.D., Dias, J.M., Brito, A.C., 2023. Climate change in estuarine systems: patterns and gaps using a meta-analysis approach. Sci. Total Environ. 858, 159742. https://doi.org/10.1016/j.scitotenv.2022.159742.

Brito, P., 2009. Impactos da elevação do nível médio do mar em ambientes costeiros: O caso do estuário do Sado. (PhD Thesis,).University of Lisbon.

Brito, A.C., Pereira, H., Picado, A., Cruz, J., Cereja, R., Biguino, B., Chainho, P., Nascimento, Â., Carvalho, F., Cabral, S., Santos, C., Palma, C., Borges, C., Dias, J.M., 2023. Increased oyster aquaculture in the Sado Estuary (Portugal): how to ensure ecosystem sustainability? Sci. Total Environ. 158898. https://doi.org/10.1016/j.scitotenv.2022.158898.

Cabral, H.N., 2000. Distribution and abundance patterns of flatfishes in the Sado Estuary, Portugal. Estuaries 23, 351. https://doi.org/10.2307/1353327.

Caeiro, S., Costa, M.H., Ramos, T.B., Fernandes, F., Silveira, N., Coimbra, A., Medeiros, G., Painho, M., 2005. Assessing heavy metal contamination in Sado Estuary sediment: an index analysis approach. Ecol. Indic. 5, 151–169. https://doi.org/10.1016/j.ecolind.2005.02.001.

Carreira, S., Costa, P.M., Martins, M., Lobo, J., Costa, M.H., Caeiro, S., 2013. Ecotoxicological heterogeneity in transitional coastal habitats assessed through the integration of biomarkers and sediment-contamination profiles: a case study using a commercial clam. Arch. Environ. Contam. Toxicol. 64, 97–109. https://doi.org/10.1007/s00244-012-9812-1.

Carroll, M.L., Johnson, B.J., Henkes, G.A., McMahon, K.W., Voronkov, A., Ambrose, W.G., Denisenko, S.G., 2009. Bivalves as indicators of environmental variation and potential anthropogenic impacts in the southern Barents Sea. Mar. Pollut. Bull. Environ. Rec. Anthropogenic Impacts Coast. Ecosyst. 59, 193–206. https://doi.org/10.1016/j.marpolbul.2009.02.022.

Carvalho, D., Rocha, A., Costoya, X., deCastro, M., Gómez-Gesteira, M., 2021. Wind energy resource over Europe under CMIP6 future climate projections: what changes from CMIP5 to CMIP6. Renew. Sust. Energ. Rev. 151, 111594. https://doi.org/10.1016/j.rser.2021.111594.

Coutinho, M.T.C.P., 2003. Comunidade Fitoplanctónica Do Estuário Do Sado: Estrutura, Dinâmica e Aspectos Ecológicos; Instituto Nacional de Investigação Agrária e das Pescas. IPIMAR 328.

Cravo, A., Rosa, A., Jacob, J., Correia, C., 2020. Dissolved oxygen dynamics in Ria Formosa Lagoon (South Portugal) - a real time monitoring station observatory. Mar. Chem. 223, 103806. https://doi.org/10.1016/j.marchem.2020.103806.

de Pablo, H., Sobrinho, J., Nunes, S., Correia, A., Neves, R., Gaspar, M.B., 2022. Climatology and nutrient fluxes in the Tagus estuary: a coupled model application. Estuar. Coast. Shelf Sci. 279, 108129. https://doi.org/10.1016/j.ecss.2022.108129.

Declerck, A., Delpey, M., Rubio, A., Ferrer, L., Basurko, O.C., Mader, J., Louzao, M., 2019. Transport of floating marine litter in the coastal area of the south-eastern Bay of Biscay: a Lagrangian approach using modelling and observations. J. Oper. Oceanogr. 12, S111–S125. https://doi.org/10.1080/1755876X.2019.1611708.

Dekker, R., Beukema, J.J., 1999. Relations of summer and winter temperatures with dynamics and growth of two bivalves, Tellina tenuis and Abra tenuis, on the northern edge of their intertidal distribution. J. Sea Res. 42, 207–220. https://doi.org/10.1016/S1385-1101(99)00026-X.

Deltares, 2014. D-Water Quality: Versatile Water Quality Modelling in 1D, 2D or 3D Systems Including Physical, (bio)Chemical and Biological Processes (User Manual). 4.99.34158. ed. Deltares, Delft.

Deltares, 2018. D-Water Quality: Processes Library Description (Technical Reference Manual). 5.01. ed. Deltares, Delft.

Deltares, 2021. Delft3D-Flow: Simulation of Multi-dimensional Hydrodynamic Flows and Transport Phenomena, Including Sediments (User Manual). 3.15. ed. Deltares, Delft.

Des, M., deCastro, M., Sousa, M.C., Dias, J.M., Gómez-Gesteira, M., 2019. Hydrodynamics of river plume intrusion into an adjacent estuary: the Minho River and Ria de Vigo. J. Mar. Syst. 189, 87–97. https://doi.org/10.1016/j.jmarsys.2018.10.003.

Des, M., Gómez-Gesteira, M., deCastro, M., Gómez-Gesteira, L., Sousa, M.C., 2020. How can ocean warming at the NW Iberian Peninsula affect mussel aquaculture? Sci. Total Environ. 709, 136117. https://doi.org/10.1016/j.scitotenv.2019.136117.

Des, M., Gómez-Gesteira, J.L., deCastro, M., Iglesias, D., Sousa, M.C., ElSerafy, G., Gómez-Gesteira, M., 2022. Historical and future naturalization of Magallana gigas in the Galician coast in a context of climate change. Sci. Total Environ. 838, 156437. https://doi.org/10.1016/j.scitotenv.2022.156437.

Dias, J.M., Lopes, J.F., Dekeyser, I., 2000. Tidal propagation in Ria de Aveiro Lagoon, Portugal. Phys. Chem. Earth B Hydrol. Oceans Atmos. 25, 369–374. https://doi.org/10.1016/S1464-1909(00)00028-9.

Dias, J.M., Pereira, F., Picado, A., Lopes, C.L., Pinheiro, J.P., Lopes, S.M., Pinho, P.G., 2021. A comprehensive estuarine hydrodynamics-salinity study: impact of morphologic changes on Ria de Aveiro (Atlantic Coast of Portugal). J. Mar. Sci. Eng. 9, 234. https://doi.org/10.3390/jmse9020234.

Dynamic Solutions, LLC, 2013. Lake Thunderbird Report for Nutrient, Turbidity, and Dissolved Oxygen TMDLs.

FAO, 2022. The State of World Fisheries and Aquaculture 2022. Towards Blue Transformation. FAO, Rome https://doi.org/10.4060/cc0461en.

Ferreira, J.G., Simas, T., Nobre, A., Silva, M., Shifferegger, K., Lencart e Silva, J., 2003. Identification of Sensitive Areas and Vulnerable Zones in Transitional and Coastal Portuguese Systems. INAG - Instituto da Água and IMAR - Institute of Marine Research, Lisbon, Portugal.

Ferreira, J.G., Abreu, P.F., Bettencourt, A.M., Bricker, S.B., Marques, J.C., Melo, J.J., Newton, A., Nobre, A., Patrício, J., Rocha, F., Rodrigues, R., Salas, F., Silva, M.C., Simas, T., Soares, C.V., Stacey, P.E., Vale, C., de Wit, M., Wolff, W.J., 2005. Monitoring Plan For Water Quality and Ecology for Portuguese Transitional and Coastal Waters. INAG (Instituto da Água) and IMAR (Institute of Marine Research).

Ferreira, J.G., Hawkins, A.J.S., Monteiro, P., Service, M., Moore, H., Edwards, A., Gowen, R., Lourenço, P., Mellor, A., Nunes, J.P., Pascoe, P.L., Ramos, L., Sequeira, A., Simas, T., Strong, J., 2007. SMILE - Sustainable Mariculture in Northern Irish Lough Ecosystems - Assessment of Carrying Capacity for Environmentally Sustainable Shellfish Culture in Carlingford Lough, Strangford Lough, Belfast Lough. Larne Lough and Lough Foyle. IMAR - Institute of Marine Research.

Filgueira, R., Guyondet, T., Comeau, L.A., Tremblay, R., 2016. Bivalve aquaculture-environment interactions in the context of climate change. Glob. Chang. Biol. 22, 3901–3913. https://doi.org/10.1111/gcb.13346.

Fraysse, M., Pinazo, C., Faure, V.M., Fuchs, R., Lazzari, P., Raimbault, P., Pairaud, I., 2013. Development of a 3D coupled physical-biogeochemical model for the Marseille coastal area (NW Mediterranean Sea): what complexity is required in the coastal zone? PLoS One 8, 1–18. https://doi.org/10.1371/journal.pone.0080012.

Freitas, D., Gomes, J., Luis, T.S., Madruga, L., Marques, C., Baptista, G., Rosalino, L.M., Antunes, P., Santos, R., Santos-Reis, M., 2007. Otters and fish farms in the Sado estuary: ecological and socio-economic basis of a conflict. Hydrobiologia 587, 51–62. https://doi.org/10.1007/s10750-007-0693-7.

Freitas, M., Andrade, C., Cruces, A., Munhá, J., Sousa, M., Moreira, S., Jouanneau, J., Martins, L., 2008. Anthropogenic influence in the Sado estuary (Portugal): a geochemical approach. J. Iber. Geol. 34.

Gomes, D., 2019. GIS-based Site Selection and Dynamic Modelling of Magallana Oyster in the Sado Estuary. Portugal (MSc Thesis).Universidade Nova de Lisboa.

Helmuth, B., Mieszkowska, N., Moore, P., Hawkins, S.J., 2006. Living on the edge of two changing worlds: forecasting the responses of rocky intertidal ecosystems to climate change. Annu. Rev. Ecol. Evol. Syst. 37, 373–404.

Iglesias, I., Bio, A., Melo, W., Avilez-Valente, P., Pinho, J., Cruz, M., Gomes, A., Vieira, J., Bastos, L., Veloso-Gomes, F., 2022. Hydrodynamic model ensembles for climate change projections in estuarine regions. Water 14, 1966. https://doi.org/10.3390/w14121966.

IPCC, 2021. In: Masson-Delmotte, V., Zhai, P., Pirani, A., Connors, S.L., Péan, C., Berger, S., Caud, N., Chen, Y., Goldfarb, L., Gomis, M.I., Huang, M., Leitzell, K., Lonnoy, E., Matthews, J.B.R., Maycock, T.K., Waterfield, T., Yelekçi, O., Yu, R., Zhou, B. (Eds.), Climate Change 2021: The Physical Science Basis. Contribution of Working Group I to the Sixth Assessment Report of the Intergovernmental Panel on Climate Change. Cambridge University Press, Cambridge, United Kingdom and New York, NY, USA.

Ishihi, Y., Matsumoto, T., Watanabe, S., Fujioka, Y., Hasegawa, N., Higano, J., 2017. Growth and food sources of asari clam Ruditapes philippinarum in suspended culture. J. Fish. Technol. 9, 141–145.

Jungclaus, J.H., Fischer, N., Haak, H., Lohmann, K., Marotzke, J., Matei, D., Mikolajewicz, U., Notz, D., von Storch, J.S., 2013. Characteristics of the ocean simulations in the Max Planck Institute Ocean Model (MPIOM) the ocean component of the MPI-Earth system model. J. Adv. Model. Earth Syst. 5, 422–446. https://doi.org/10.1002/jame.20023.

Laurent, A., Fennel, K., Kuhn, A., 2021. An observation-based evaluation and ranking of historical Earth system model simulations in the northwest North Atlantic Ocean. Biogeosciences 18, 1803–1822. https://doi.org/10.5194/bg-18-1803-2021.

Leal Filho, W., Nagy, G.J., Martinho, F., Saroar, M., Erache, M.G., Primo, A.L., Pardal, M.A., Li, C., 2022. Influences of climate change and variability on estuarine ecosystems: an impact study in selected European, south American and Asian countries. Int. J. Environ. Res. Public Health 19, 585. https://doi.org/10.3390/ijerph19010585.

Lee, H.-M., Kim, H.-J., Park, K.-I., Choi, K.-S., 2020. Enhanced growth, gonad maturation, and low-level parasite infection in juvenile Manila clam Ruditapes philippinarum cultured in subtidal cages on the south coast of Korea. Aquaculture 526, 735410. https://doi.org/10.1016/j.aquaculture.2020.735410.

Lillebø, A.I., Coelho, P.J., Pato, P., Válega, M., Margalho, R., Reis, M., Raposo, J., Pereira, E., Duarte, A.C., Pardal, M.A., 2011. Assessment of mercury in water, sediments and biota of a Southern European Estuary (Sado Estuary, Portugal). Water Air Soil Pollut. 214, 667–680. https://doi.org/10.1007/s11270-010-0457-2.

Liu, W., He, M., 2012. Effects of ocean acidification on the metabolic rates of three species of bivalve from southern coast of China. Chin. J. Oceanol. Limnol. 30, 206–211. https://doi.org/10.1007/s00343-012-1067-1.

Lopes, C., 2016. Flood Risk Assessment in Ria de Aveiro under Present and Future Scenarios. (PhD Thesis,).University of Aveiro.

Lopes, C.L., Sousa, M.C., Ribeiro, A., Pereira, H., Pinheiro, J.P., Vaz, L., Dias, J.M., 2022. Evaluation of future estuarine floods in a sea level rise context. Sci. Rep. 12, 8083. https://doi.org/10.1038/s41598-022-12122-7.

Lorente, P., Piedracoba, S., Sotillo, M.G., Aznar, R., Amo-Baladrón, A., Pascual, Á., Soto-Navarro, J., Álvarez-Fanjul, E., 2016. Ocean model skill assessment in the NW Mediterranean using multi-sensor data. J. Oper. Oceanogr. 9, 75–92. https://doi.org/10.1080/1755876X.2016.1215224.

Maretec, C., 2002. Water Quality in Portuguese Estuaries (Tejo-Sado-Mondego). Instituto Superior Técnico (IST).

Marshall, R.D., Dunham, A., 2013. Effects of culture media and stocking density on biofouling, shell shape, growth, and survival of the Pacific oyster (Crassostrea gigas) and the Manila clam (Venerupis philippinarum) in suspended culture. Aquaculture 406–407, 68–78. https://doi.org/10.1016/j.aquaculture.2013.05.003.

Marta-Almeida, M., Teixeira, J.C., Carvalho, M.J., Melo-Gonçalves, P., Rocha, A.M., 2016. High resolution WRF climatic simulations for the Iberian Peninsula: model validation. Physics and Chemistry of the Earth, Parts A/B/C, 3rd International Conference on Ecohydrology, Soil and Climate Change, EcoHCC'14 94, pp. 94–105 https://doi.org/10.1016/j.pce.2016.03.010.

Martins, F., Leitão, P., Silva, A., Neves, R., 2001. 3D modelling in the Sado estuary using a new generic vertical discretization approach. Oceanol. Acta 24, 51–62. https://doi.org/10.1016/S0399-1784(01)00092-5.

Martins, F., Leitão, P., Neves, R., 2002. Simulating vertical water mixing in homogeneous estuaries: the SADO Estuary case. In: Orive, E., Elliott, M., de Jonge, V.N. (Eds.), Nutrients and Eutrophication in Estuaries and Coastal Waters. Springer, Netherlands, Dordrecht, pp. 221–227 https://doi.org/10.1007/978-94-017-2464-7_19.

Masson, D., Peña, A., 2009. Chlorophyll distribution in a temperate estuary: the Strait of Georgia and Juan de Fuca Strait. Estuar. Coast. Shelf Sci. 82, 19–28. https://doi.org/10.1016/j.ecss.2008.12.022.

Mateus, M., Neves, R., 2008. Evaluating light and nutrient limitation in the Tagus estuary using a process-oriented ecological model. J. Mar. Eng. Technol. 7, 43–54. https://doi.org/10.1080/20464177.2008.11020213.

Mateus, M., Vaz, N., Neves, R., 2012. A process-oriented model of pelagic biogeochemistry for marine systems. Part II: application to a mesotidal estuary. J. Mar. Syst. Remote Sens. Math. Model. In-situ Data Improv. Coast. Manag. Supporting Tools 94, S90–S101. https://doi.org/10.1016/j.jmarsys.2011.11.009.

Mendes, J., Ruela, R., Picado, A., Pinheiro, J.P., Ribeiro, A.S., Pereira, H., Dias, J.M., 2021. Modeling dynamic processes of Mondego Estuary and Óbidos lagoon using Delft3D. JMSE 9, 91. https://doi.org/10.3390/jmse9010091.

Miranda, P.M.A., Alves, J.M.R., Serra, N., 2013. Climate change and upwelling: response of Iberian upwelling to atmospheric forcing in a regional climate scenario. Clim. Dyn. 40, 2813–2824. https://doi.org/10.1007/s00382-012-1442-9.

MMO, 2019. Identification of Areas of Aquaculture Potential in English Waters (Project No: 1184). A Report Produced for the Marine Management Organisation by Centre for Environment Fisheries and Aquaculture Science.

Nascimento, Â., Biguino, B., Borges, C., Cereja, R., Cruz, J.P.C., Sousa, F., Dias, J., Brotas, V., Palma, C., Brito, A.C., 2021. Tidal variability of water quality parameters in a mesotidal estuary (Sado Estuary, Portugal). Sci. Rep. 11, 23112. https://doi.org/10.1038/s41598-021-02603-6.

Pereira, H., Sousa, M.C., Vieira, L.R., Morgado, F., Dias, J.M., 2022. Modelling salt intrusion and estuarine plumes under climate change scenarios in two transitional ecosystems from the NW Atlantic Coast. J. Mar. Sci. Eng. 10, 262. https://doi.org/10.3390/jmse10020262.

Picado, A., Oliveira, V., Pereira, H., Sousa, M.C., Costa, L., Almeida, A., Dias, J.M., 2020. Assessing the potential of Minho and Lima Estuaries for aquaculture. J. Coast. Res. 95, 148. https://doi.org/10.2112/SI95-029.1.

Psuty, N.P., Moreira, M.E.S.A., 2000. Holocene sedimentation and sea level rise in the Sado Estuary, Portugal. J. Coast. Res. 16, 125–138.

Rato, A., Joaquim, S., Matias, A.M., Roque, C., Marques, A., Matias, D., 2022. The impact of climate change on bivalve farming: combined effect of temperature and salinity on survival and feeding behavior of clams Ruditapes decussatus. Front. Mar. Sci. 9, 932310. https://doi.org/10.3389/fmars.2022.932310.

Reale, M., Giorgi, F., Solidoro, C., Di Biagio, V., Di Sante, F., Mariotti, L., Farneti, R., Sannino, G., 2020. The regional earth system model RegCM-ES: evaluation of the Mediterranean climate and marine biogeochemistry. J. Adv. Model. Earth Syst. 12, e2019MS001812. https://doi.org/10.1029/2019MS001812.

Ribeiro, A.S., Sousa, M.C., Lencart e Silva, J.D., Dias, J.M., 2016. David and Goliath revisited: joint modelling of the Tagus and Sado Estuaries. J. Coast. Res. 75, 123–127. https://doi.org/10.2112/SI75-025.1.

Robins, P.E., Skov, M.W., Lewis, M.J., Giménez, L., Davies, A.G., Malham, S.K., Neill, S.P., McDonald, J.E., Whitton, T.A., Jackson, S.E., Jago, C.F., 2016. Impact of climate change on UK estuaries: a review of past trends and potential projections. Estuar. Coast. Shelf Sci. 169, 119–135. https://doi.org/10.1016/j.ecss.2015.12.016.

Rodrigues, A.M.J., Quintino, V.M.S., 1993. Horizontal biosedimentary gradients across the Sado estuary, W. Portugal. Neth. J. Aquat. Ecol. 27, 449–464. https://doi.org/10.1007/BF02334806.

Rodrigues, M., Rosa, A., Cravo, A., Jacob, J., Fortunato, A.B., 2021. Effects of climate change and anthropogenic pressures in the water quality of a coastal lagoon (Ria Formosa, Portugal). Sci. Total Environ. 780, 146311. https://doi.org/10.1016/j.scitotenv.2021.146311.

Santos, M., Amorim, A., Brotas, V., Cruz, J.P.C., Palma, C., Borges, C., Favareto, L.R., Veloso, V., Dâmaso-Rodrigues, M.L., Chainho, P., Félix, P.M., Brito, A.C., 2022. Spatio-temporal dynamics of phytoplankton community in a well-mixed temperate estuary (Sado Estuary, Portugal). Sci. Rep. 12, 16423. https://doi.org/10.1038/s41598-022-20792-6.

Sent, G., Biguino, B., Favareto, L., Cruz, J., Sá, C., Dogliotti, A.I., Palma, C., Brotas, V., Brito, A.C., 2021. Deriving water quality parameters using sentinel-2 imagery: a case study in the Sado estuary. Portugal. Remote Sens. 13. https://doi.org/10.3390/rs13051043.

Sobral, M.P., 1995. Ecophysiology of Ruditapes Decussatus. (PhD Thesis,).University of Lisbon, Lisbon, Portugal.

Sousa, M.C., Ribeiro, A.S., Des, M., Mendes, R., Alvarez, I., Gomez-Gesteira, M., Dias, J.M., 2018. Integrated high-resolution numerical model for the NW Iberian Peninsula coast and main estuarine systems. coas 85, 66–70. https://doi.org/10.2112/SI85-014.1.

Steeves, L.E., Filgueira, R., Guyondet, T., Chassé, J., Comeau, L., 2018. Past, present, and future: performance of two bivalve species under changing environmental conditions. Front. Mar. Sci. 5.

Stevens, A., Gobler, C., 2018. Interactive effects of acidification, hypoxia, and thermal stress on growth, respiration, and survival of four North Atlantic bivalves. Mar. Ecol. Prog. Ser. 604, 143–161. https://doi.org/10.3354/meps12725.

Subasinghe, R., Soto, D., Jia, J., 2009. Global aquaculture and its role in sustainable development. Rev. Aquac. 1, 2–9. https://doi.org/10.1111/j.1753-5131.2008.01002.x.

Thiyagarajan, V., Ko, G.W.K., 2012. Larval growth response of the Portuguese oyster (Crassostrea angulata) to multiple climate change stressors. Aquaculture 370–371, 90–95. https://doi.org/10.1016/j.aquaculture.2012.09.025.

Truesdale, G.A., Downing, A.L., Lowden, G.F., 1955. The solubility of oxygen in pure water and seawater. J. Appl. Chem. 5, 53–62. https://doi.org/10.1002/jctb.5010050201.

Vale, C., Cortesão, C., Castro, O., Ferreira, A.M., 1993. Suspended-sediment response to pulses in river flow and semidiurnal and fortnightly tidal variations in a mesotidal estuary. Marine Chemistry, Second International Symposium on the Biogeochemistry of Model Estuaries: Estuarine Processes in Global Change. 43, pp. 21–31. https://doi.org/10.1016/0304-4203(93)90213-8.

Vaz, N., Mateus, M., Plecha, S., Sousa, M.C., Leitão, P.C., Neves, R., Dias, J.M., 2015. Modeling SST and chlorophyll patterns in a coupled estuary-coastal system of Portugal: the Tagus case study. Journal of Marine Systems, The variability of primary production in the ocean: From the synoptic to the global scale. The 45th International Liege Colloquium on Ocean Dynamics, Liege, Belgium, May 13-17, 2013 147, pp. 123–137 https://doi.org/10.1016/j.jmarsys.2014.05.022.

Vaz, L., Frankenbach, S., Serôdio, J., Dias, J.M., 2019. New insights about the primary production dependence on abiotic factors: Ria de Aveiro case study. Ecol. Indic. 106, 105555. https://doi.org/10.1016/j.ecolind.2019.105555.

Vaz, L., Sousa, M.C., Gómez-Gesteira, M., Dias, J.M., 2021. A habitat suitability model for aquaculture site selection: Ria de Aveiro and Rias Baixas. Sci. Total Environ. 801, 149687. https://doi.org/10.1016/j.scitotenv.2021.149687.

Wang, H., Chen, Q., Hu, K., La Peyre, M.K., 2017. A modeling study of the impacts of Mississippi River diversion and sea-level rise on water quality of a deltaic estuary. Estuar. Coasts 40, 1028–1054. https://doi.org/10.1007/s12237-016-0197-7.

Williams, J.J., Esteves, L.S., 2017. Guidance on setup, calibration, and validation of hydrodynamic, wave, and sediment models for shelf seas and estuaries. Adv. Civil Eng. 2017, 1–25. https://doi.org/10.1155/2017/5251902.

Woods, H.A., Makino, W., Cotner, J.B., Hobbie, S.E., Harrison, J.F., Acharya, K., Elser, J.J., 2003. Temperature and the chemical composition of poikilothermic organisms. Funct. Ecol. 17, 237–245. https://doi.org/10.1046/j.1365-2435.2003.00724.x.

Xu, J., Hood, R.R., 2006. Modeling biogeochemical cycles in Chesapeake Bay with a coupled physical–biological model. Estuar. Coast. Shelf Sci. 69, 19–46. https://doi.org/10.1016/j.ecss.2006.03.021.

Xue, H., Chai, F., 2012. Coupled Physical-Biological Model for the Pearl River Estuary: A Phosphate Limited Subtropical Ecosystem 913–928. https://doi.org/10.1061/40628(268)58.

Zijl, F., Laan, S.C., Emmanouil, A., Kessel, T., Zelst, V.T.M., Vilmin, L.M., Duren, L.A., 2021. Potential Ecosystem Effects of Large Upscaling of Offshore Wind in the North Sea.